RESEARCH ARTICLE

Bazooka inhibits aPKC to limit antagonism of actomyosin networks during amnioserosa apical constriction

Daryl J. V. David[1], Qiming Wang[2], James J. Feng[2,3] and Tony J. C. Harris[1,*]

ABSTRACT

Cell shape changes drive tissue morphogenesis during animal development. An important example is the apical cell constriction that initiates tissue internalisation. Apical constriction can occur through a phase of cyclic assembly and disassembly of apicomedial actomyosin networks, followed by stabilisation of these networks. Delayed negative-feedback mechanisms typically underlie cyclic behaviour, but the mechanisms regulating cyclic actomyosin networks remain obscure, as do mechanisms that transform overall network behaviour. Here, we show that a known inhibitor of apicomedial actomyosin networks in *Drosophila* amnioserosa cells, the Par-6-aPKC complex, is recruited to the apicomedial domain by actomyosin networks during dorsal closure of the embryo. This finding establishes an actomyosin-aPKC negative-feedback loop in the system. Additionally, we find that aPKC recruits Bazooka to the apicomedial domain, and phosphorylates Bazooka for a dynamic interaction. Remarkably, stabilising aPKC-Bazooka interactions can inhibit the antagonism of actomyosin by aPKC, suggesting that Bazooka acts as an aPKC inhibitor, and providing a possible mechanism for delaying the actomyosin-aPKC negative-feedback loop. Our data also implicate an increasing degree of Par-6-aPKC-Bazooka interactions as dorsal closure progresses, potentially explaining a developmental transition in actomyosin behaviour from cyclic to persistent networks. This later impact of aPKC inhibition is supported by mathematical modelling of the system. Overall, this work illustrates how shifting chemical signals can tune actomyosin network behaviour during development.

KEY WORDS: Apical constriction, Par proteins, Actomyosin networks

INTRODUCTION

For animal development and tissue morphogenesis, cells must change shape. For example, the invagination of epithelial sheets is initiated by apical cell constriction (Martin, 2010; Sawyer et al., 2010; Harris, 2012; Suzuki et al., 2012). Non-muscle myosin II (hereafter myosin) pulling on filamentous actin (F-actin) provides the major contractile forces in such cells. With linkage to plasma membrane complexes, such contractility can change cell shape, and with linkage to adherens junctions (AJs), the contractility also pulls on neighbouring cells for coordinated tissue morphogenesis.

In many models of apical constriction, such as the *Drosophila* ventral furrow (Martin et al., 2009), the *Drosophila* amnioserosa at

[1]Department of Cell and Systems Biology, University of Toronto, Toronto, Ontario, M5S 3G5, Canada. [2]Department of Mathematics, University of British Columbia, Vancouver, British Columbia, V6T 1Z2, Canada. [3]Department of Chemical and Biological Engineering, University of British Columbia, Vancouver, British Columbia, V6T 1Z3, Canada.

*Author for correspondence (tony.harris@utoronto.ca)

dorsal closure (DC) (Blanchard et al., 2010; David et al., 2010) and *Caenorhabditis elegans* mesodermal precursor cells (Munro et al., 2004; Roh-Johnson et al., 2012), apical actomyosin networks form webs across the apical domain. Additionally, the networks display a range of dynamic properties, with pulsatile, flowing and/or persistent elements. These network properties lead to distinctive apical constriction mechanisms in the different cell types, and the networks can change their properties during development. However, mechanisms regulating these network properties, and their changes, are poorly understood.

Cyclic assembly and disassembly of actomyosin networks should obey general principles governing cyclic signalling (Ferrell et al., 2011; Lim et al., 2013). From studies of the cell cycle, circadian rhythms and other systems, the principle of delayed negative feedback has emerged. With an activating input signal, there are two responses: (1) the output response and (2) a delayed inhibition of the input signal. After signalling from the input, the output occurs followed by the delayed input inhibition, which leads to loss of both the output and the negative feedback. If the input signal is continually available, the cycle will repeat ad infinitum.

For actomyosin networks, many activating inputs are known [e.g. Rho family small GTPases and downstream actin nucleation promoting factors, actin elongation factors, and myosin activating kinases (Chhabra and Higgs, 2007; Pollard, 2007)], but we are just beginning to understand mechanisms of delayed negative feedback that could promote network assembly-disassembly cycles. Delayed negative feedback could arise physically or chemically (Kruse and Riveline, 2011; Levayer and Lecuit, 2012). For example, myosin contractility can depolymerise F-actin *in vitro*, suggesting a mechanism of delayed negative feedback in which actomyosin network assembly leads to myosin contractility and subsequent network disassembly. Alternatively, cyclic actomyosin activity has been shown to be entrained by cyclic calcium signalling in cell culture.

During *Drosophila* DC, amnioserosa cells provide an excellent model of apical constriction (Gorfinkiel and Blanchard, 2011; Harris, 2012). Midway through embryogenesis, the squamous epithelium formed by these cells becomes covered by the surrounding epidermis. One way the amnioserosa contributes to this internalisation is by undergoing apical constriction. Indeed, apical constriction of amnioserosa cells is sufficient to drive DC (Franke et al., 2005). During early DC, the apical constriction of amnioserosa cells is oscillatory and is driven by the cyclic assembly and disassembly of apical actomyosin networks (Solon et al., 2009; Blanchard et al., 2010; David et al., 2010). During later DC, amnioserosa cell oscillations are dampened in magnitude (Solon et al., 2009; Blanchard et al., 2010; Sokolow et al., 2012), and this change coincides with increased levels of activated (phosphorylated) apical myosin (Blanchard et al., 2010). Thus, the amnioserosa provides a model for studying cyclic actomyosin networks and potentially for studying the dampening of such cycling. Recent

mathematical modelling showed that amnioserosa cells can undergo sustained oscillations through (1) cell-autonomous feedback loops in which a hypothetical signal activates myosin and is then depleted with myosin activity, and (2) mechanical coupling between neighbouring cells (Wang et al., 2012). However, the cell-autonomous signalling mechanisms remain obscure, and the model was not able to explain the dampening of cell oscillations at late DC.

Proteins of the Partitioning defective (Par) complex regulate the cycling of amnioserosa actomyosin networks (David et al., 2010). The Par complex controls various aspects of cell polarity across a wide range of cell types from nematodes to flies to humans. It is composed of Par-3 [Bazooka (Baz) in *Drosophila*], Par-6 and atypical Protein Kinase C (aPKC). However, the complex is dynamic with Par-6-aPKC complexes often acting separately from Par-3/Baz (Goldstein and Macara, 2007; St Johnston and Ahringer, 2010; Tepass, 2012). Indeed, during amnioserosa apical constriction, Baz promotes actomyosin networks whereas Par-6-aPKC complexes inhibit the networks (David et al., 2010). Here, we show that actomyosin networks recruit Par-6-aPKC complexes to the apical domain, suggesting a negative-feedback loop. aPKC acts in turn to recruit Baz, and Baz promotes apical constriction by inhibiting Par-6-aPKC activity. Our data suggest that this inhibition increases during DC, providing a mechanism that could induce the transition from cyclic to persistent actomyosin networks by late DC, an idea supported by mathematical modelling.

RESULTS

Amnioserosa apicomedial actomyosin networks become more persistent at later dorsal closure

Amnioserosa apical constriction occurs in two main phases. During earlier DC, apical domains are oscillatory owing to the pulsatile assembly and disassembly of actomyosin networks (Solon et al., 2009; Blanchard et al., 2010; David et al., 2010). During later DC, amnioserosa cell oscillations are dampened (Solon et al., 2009; Blanchard et al., 2010; Sokolow et al., 2012). This change coincides with increased levels of phosphorylated myosin regulatory light chain over the apical domain (Blanchard et al., 2010), suggesting that more persistent actomyosin networks account for the dampened cell dynamics. However, apical pulses of GFP-tagged myosin regulatory light chain were previously observed after substantial apical constriction and reduced cell oscillation (David et al., 2010). These later pulses were accompanied by a separate increase in the GFP-tagged protein around the apical circumference of amnioserosa cells (David et al., 2010). As this apical circumferential distribution was not detected when the phosphorylated form of the endogenous protein was probed (Blanchard et al., 2010), we suspected that the GFP-tagged protein may have abnormal properties. Thus, we used two different probes to assess actomyosin network dynamics at late DC.

To investigate further whether cytoskeletal stabilisation could account for the reduced cell oscillation at DC, we live imaged the GFP-tagged actin-binding domain of moesin (moeABD::GFP), and a GFP-tagged form of non-muscle myosin II heavy chain [Zipper (Zip)] expressed in a gene trap line with GFP inserted into the endogenous *zip* locus. At early DC, both probes revealed pulsatile networks over the apicomedial cortex of amnioserosa cells (Fig. 1A,B; supplementary material Movies 1, 2). moeABD::GFP also localised to protrusions around the apical circumference and to cell-cell junctions. By contrast, by late DC, both probes revealed more persistent actomyosin networks over the apicomedial cortex of amnioserosa cells (Fig. 1A,B; supplementary material Movies 1, 2). Thus, amnioserosa apicomedial actomyosin networks become more persistent at later DC.

Par proteins progressively shift apicomedially over dorsal closure

Because Baz and Par-6-aPKC help coordinate the pulsing of early actomyosin networks, we hypothesised that they might also affect the transition to more persistent networks. Thus, we compared Par protein localisation between early and late DC in fixed and live samples. During early DC, fixation and staining for Baz, aPKC and a Par-6::GFP construct (expressed under the control of the *par-6* promoter in a *par-6* mutant background) revealed a punctate distribution over the apical surface of amnioserosa cells, in addition to circumferential staining, for each protein (Fig. 2A,C,E), as seen previously (David et al., 2010). The circumferential staining was greater for Baz in the fixed samples, but live imaging of the Par-6::GFP construct and Baz::GFP (expressed in a gene trap line with GFP inserted into the endogenous *baz* locus) revealed similar patterns of apicomedial and apical circumferential puncta (Fig. 2G,H), indicating that the detection of circumferential Par-6-aPKC is altered by fixation at this stage. By contrast, by late DC, all probes, fixed or live, revealed a striking concentration of Par protein puncta over the apical surface of the cells in contrast to their apical circumferences (Fig. 2B,D,F,I,J). Of note, we observed no region-specific changes, suggesting that the re-localisations occur uniformly across the tissue. Thus, amnioserosa Par proteins progressively accumulate apicomedially as DC proceeds.

Compared with apical protein levels in the surrounding epidermis, the apicomedial Par protein levels in the amnioserosa were relatively low at early DC (Fig. 2A,C,E,G,H), but their total apicomedial levels increased substantially by late DC to generally match levels around the apical circumference of epidermal cells (Fig. 2B,D,F,I,J). However, quantification of individual puncta intensities in live images of the Par-6::GFP rescue line and the Baz::GFP trap line revealed that for each protein prominent amnioserosa apical surface puncta had similar total intensities between early and late DC (although a slight increase in the intensity of apicomedial amnioserosa Par-6::GFP puncta occurs at late DC) (Fig. 2K). Notably, the prominent Baz::GFP puncta were ~66% less intense than the prominent Par-6::GFP puncta (Fig. 2K), suggesting Baz is present at sub-stoichiometric levels compared with Par-6-aPKC complexes. Previous live imaging of co-overexpressed Par-6-GFP and Baz-mCherry revealed a mixture of overlapping and non-overlapping apicomedial puncta (David et al., 2010). To evaluate the potential for colocalisation of the Par-6::GFP and Baz::GFP constructs expressed at endogenous levels, we quantified the apical area occupied by puncta in live images taken with the same settings. Large increases in the apical surface covered by Par-6::GFP and Baz::GFP puncta occurred from early to mid-late DC (Fig. 2L). Thus, the apicomedial Par protein accumulation might be due to clustering and addition of puncta (in addition to diffuse protein), and the Par proteins have an increasing potential to interact as DC proceeds.

Amnioserosa actomyosin networks preferentially recruit aPKC

Patches of Par protein puncta continually persist at the apicomedial domain of amnioserosa cells during both the assembly and disassembly of actomyosin networks (David et al., 2010). These observations suggested that Par protein localisation does not continually rely on the actomyosin networks, but it remained possible that the networks influence the Par proteins.

To probe for immediate effects of actomyosin network assembly on the Par complex patches, we monitored patches of Baz::GFP and Par-6::GFP as amnioserosa cells constricted. During the pulsing phase of early DC, Par protein patches condensed as constriction
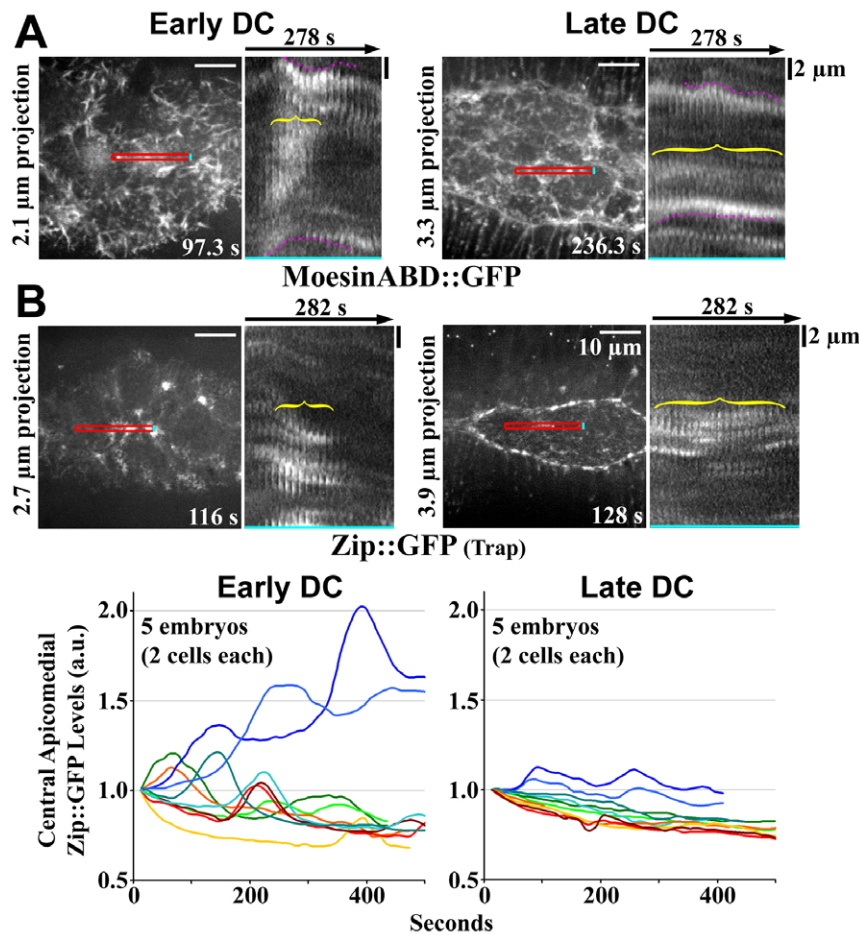
Fig. 1. A transition from pulsatile to persistent amnioserosa actomyosin networks over DC.
(A,B) MoeABD::GFP (A) and Zip::GFP (B) live at early and late DC. Red boxes outline regions of apicomedial networks depicted in kymographs, right (network durations bracketed; cell edges dot-outlined; turquoise edges of boxes are at bottoms of kymographs). Below, levels of apicomedial Zip::GFP (excluding apical circumference) are shown quantified over time for five embryos (colour-coded; two cells each) at early and late DC.

occurred (Fig. 3A; supplementary material Movies 3, 4), suggesting a local effect of actomyosin network contraction on the apical Par protein puncta. At later DC, when pulsing subsided, the Par protein patches became less dynamic (Fig. 3A; supplementary material Movies 3, 4). Thus, the Par protein patches displayed dynamic properties mirroring those of the actomyosin networks from early to late DC.

To test if the pulsing actomyosin networks are important for Par protein apical accumulation, we sought a mutant that lacks apicomedial network assembly. We hypothesised that the networks would depend on myosin, and thus analysed MoeABD::GFP in zygotic zip[1] mutants. The pulsing actin networks seen in wild type (WT) did not develop in the mutants (data not shown). To evaluate differences in aPKC and Baz levels, we co-fixed, stained and mounted the mutants with WT embryos expressing histone::GFP. The mutants displayed a marked reduction in the apical surface enrichment of aPKC and Baz, and also circumferential Baz was consistently reduced relative to the epidermis (Fig. 3B). Thus, over developmental time, the repeated assembly of actomyosin networks appears to contribute to the full recruitment of apicomedial Par proteins.

To examine how closely the Par proteins are linked to the actomyosin networks, we analysed two ectopically induced apicomedial actin networks in amnioserosa cells. First, amnioserosa overexpression of constitutively active chicken myosin light chain kinase (CA-MLCK) is known to increase apical surface myosin networks (Blanchard et al., 2010). CA-MLCK overexpression also induced abnormally compacted actin networks and cables over the apical surface of amnioserosa cells. Co-staining for aPKC revealed striking colocalisation with the ectopic actin assemblies (Fig. 3C,

arrows). By contrast, Baz displayed less direct colocalisation with the actin assemblies, displaying instead a more disperse accumulation in proximity to the actin structures (Fig. 3C, brackets). Second, we treated embryos with cytochalasin D. F-actin was lost from the leading edge of epidermal cells (Fig. 3D-G), but ectopic F-actin structures were also induced in the epidermis and amnioserosa, consistent with reports of cytochalasin D-induced actin networks (Schliwa, 1982; Mortensen and Larsson, 2003). In the epidermis, neither aPKC nor Baz was noticeably recruited to the ectopic actin structures (Fig. 3E′,G′). By contrast, both aPKC and Baz were recruited to the structures in amnioserosa cells (Fig. 3E″,G″, arrows), suggesting that the Par proteins are more susceptible to actin recruitment in the amnioserosa than in the epidermis. Although such cytochalasin D-induced actin structures are poorly understood, Zip::GFP showed exclusion from them (Fig. 3E″,G″, arrows), suggesting not all actin-associated proteins are recruited. Overall, these results reveal a unique relationship between the Par proteins and actin networks in the amnioserosa, and that this connection might be closer for aPKC than for Baz.

aPKC recruits Baz to the apicomedial domain

Because the Par proteins affect the localisation of one another in other contexts (Goldstein and Macara, 2007; St Johnston and Ahringer, 2010; Tepass, 2012), we hypothesised that their interactions would also affect their localisation in amnioserosa cells. Par-6 and aPKC directly interact and appear to act as a unit downstream of Cdc42 activation (Goldstein and Macara, 2007; St Johnston and Ahringer, 2010; Tepass, 2012). Additionally, Par-6 and aPKC interact with Baz: Par-6 binds to Baz PDZ1 (Morais-de-Sá et
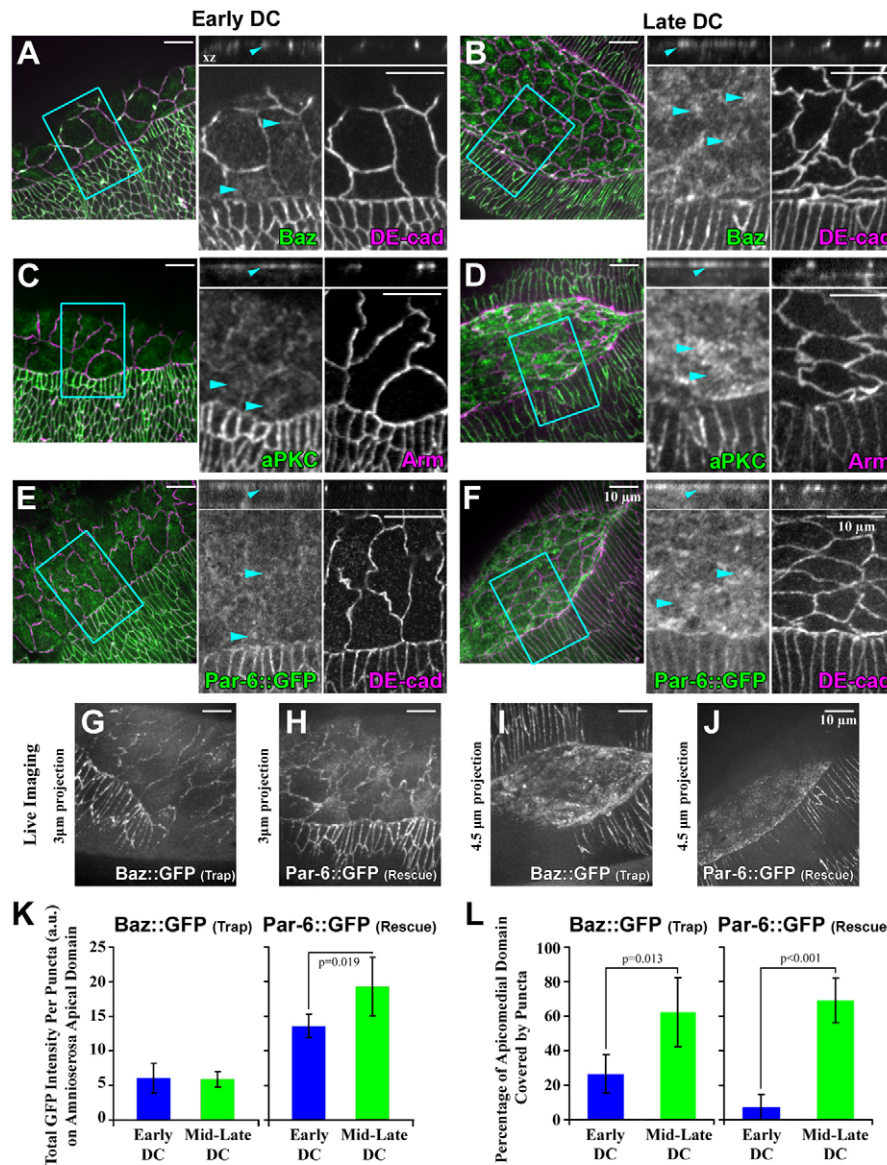
DEVELOPMENT

Fig. 2. An increase in apicomedial Par protein puncta over DC. (A-F) Fixed imaging of Baz (A,B), aPKC (C,D) and a Par-6::GFP rescue construct (E,F) at early and late DC. Boxes outline magnified regions at right (epidermis at base). Arrowheads indicate apical surface puncta. DE-cadherin staining shows cell circumferences. (G-J) Live imaging of a Baz::GFP trap line (G,I) and the Par-6::GFP rescue line (H,J) at early (G,H) and late (I,J) DC (amnioserosa central). (K) Individual Baz::GFP and Par-6::GFP puncta intensities in amnioserosa apicomedial domains in live embryos at early and mid-late DC (mean ± s.d.; n=4-6 embryos per genotype per stage). (L) Percentage of apical domain area covered by Baz::GFP and Par-6::GFP puncta in live embryos at early and mid-late DC (mean ± s.d.; n=4-6 embryos per genotype per stage).

al., 2010); aPKC binds to Baz PDZ2-3 (Wodarz et al., 2000); and aPKC additionally binds to a conserved C-terminal aPKC-binding region, which it also phosphorylates and dissociates from upon phosphorylation (Morais-de-Sá et al., 2010).

To assess how Baz affects the localisation of aPKC in amnioserosa cells, we examined zygotic baz^{Xi106} hypomorphic mutants in which maternally supplied Baz is undetectable by DC (Tanentzapf and Tepass, 2003; McKinley et al., 2012). To evaluate differences in aPKC levels, we co-fixed, stained and mounted the mutants with WT embryos expressing histone::GFP. In contrast to the WT controls, aPKC levels were markedly reduced at the apical surface of amnioserosa cells, but also in the epidermis (Fig. 4A), as reported previously (Wodarz et al., 2000). Levels of the AJ marker Armadillo were unaffected, except where epithelial structure was lost in the mutants. Thus, Baz is needed for full amnioserosa apicomedial localisation of aPKC, but this effect appears to reflect the general role of Baz in maintaining apical aPKC in all epithelial cells. Of note, a Baz::GFP construct rescued the general loss of aPKC in baz^{Xi106} zygotic mutants, but a Baz construct in which the C-terminal aPKC-binding region was deleted, $\mathrm{Baz}^{\Delta a\mathrm{PKC}}$::GFP, did not (data not shown) (McKinley et al., 2012).

To test how aPKC affects Baz in amnioserosa cells, we first analysed zygotic $apkc^{k06403}$ null mutants, but observed no effect on Baz localisation, consistent with the mutants having sufficient maternally supplied aPKC to complete embryogenesis and survive until larval stages (Rolls et al., 2003). By contrast, maternal-zygotic mutants of this and other alleles have earlier embryonic defects that would confound DC analyses (Harris and Peifer, 2007; Guilgur et al., 2012). Thus, we utilised the $\mathrm{Baz}^{\Delta a\mathrm{PKC}}$::GFP construct. To test the role of the aPKC-binding region in Baz, we expressed the deletion construct and full-length Baz at near endogenous levels in the baz^{Xi106} zygotic mutant background (McKinley et al., 2012). In the amnioserosa at early-mid DC, Baz::GFP localised to both the apical circumference and apicomedially (Fig. 4B; arrows show apicomedial localisation), as seen for endogenous Baz (Fig. 2) (David et al., 2010). By contrast, $\mathrm{Baz}^{\Delta a\mathrm{PKC}}$::GFP failed to localise apicomedially, and displayed greater enrichment around the apical circumference of amnioserosa cells (Fig. 4B). Baz::GFP and $\mathrm{Baz}^{\Delta a\mathrm{PKC}}$::GFP were indistinguishable in the epidermis, as reported previously (McKinley et al., 2012), and similar overall effects were observed in live embryos (data not shown). Thus, the C-terminal aPKC-binding region in Baz is specifically required for recruiting
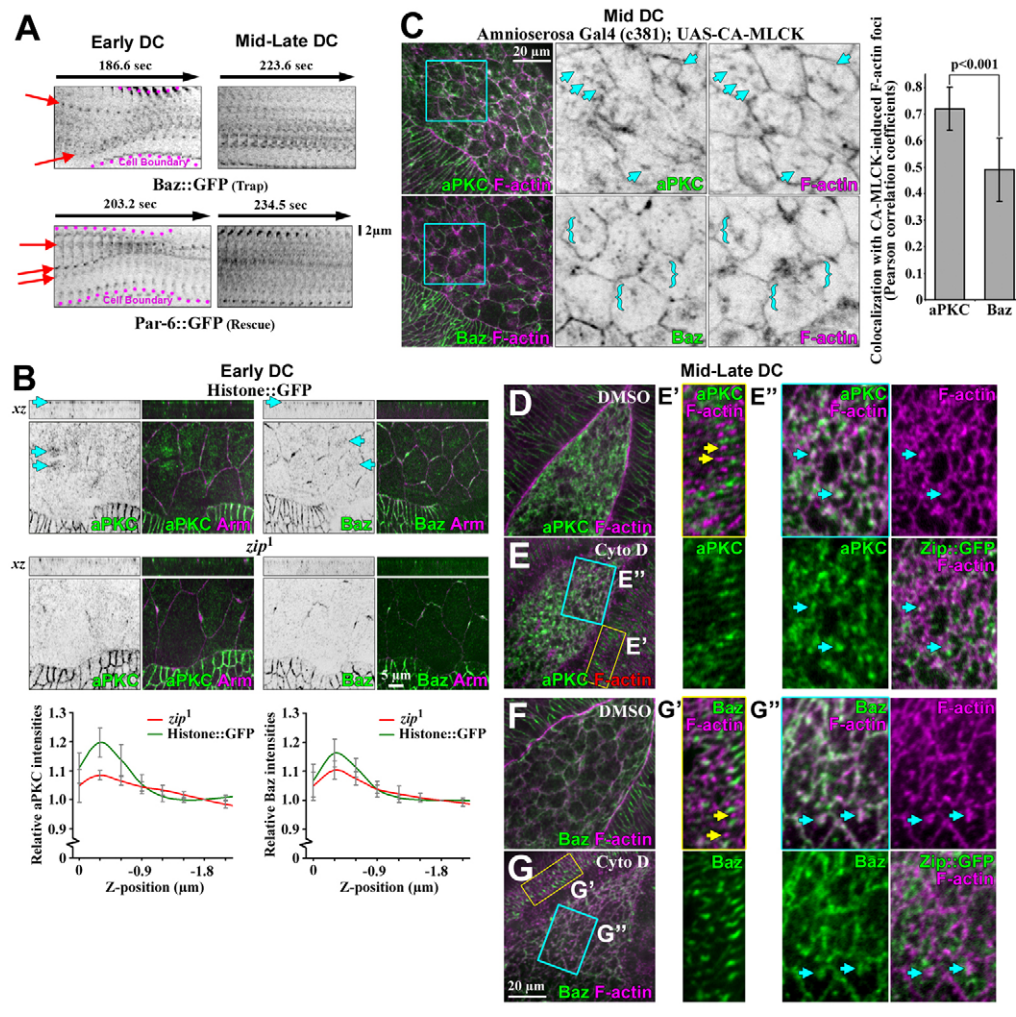
DEVELOPMENT

Fig. 3. Actomyosin activity promotes apicomedial Par protein accumulation. (A) Baz::GFP and Par-6::GFP kymographs show transient clustering of Par protein puncta as amnioserosa cells constrict at early DC (red arrows), and less puncta movement at late DC (cell edges dot-outlined). (B) aPKC and Baz amnioserosa apical surface enrichments in histone::GFP control embryos (arrows) are reduced in *zip*[1] zygotic mutants fixed, stained, mounted and imaged together. For quantification (below), data are normalised to cytoplasmic signal below apical surface (see Materials and methods; mean ± s.d.; *n*=4-7 embryos per protein per genotype). (C) aPKC, Baz and F-actin in amnioserosa cells overexpressing CA-MLCK at mid-DC. Boxes outline magnified regions at right. Ectopic F-actin structures specifically recruit aPKC (arrows) and more diffusely recruit Baz (brackets). Quantification is shown to the right (mean ± s.d.; *n*=15 cells from five embryos each). (D-G″) Effects of cytochalasin D on F-actin, aPKC and Baz at mid-late DC in the Zip::GFP trap line. (D,F) DMSO carrier controls. (E-E″,G-G″) Cytochalasin D treatments. Yellow boxes outline magnified epidermal regions (E′,G′). Turquoise boxes outline magnified amnioserosa regions (E″,G″). Ectopic F-actin structures recruit aPKC and Baz but not Zip::GFP (arrows), specifically in amnioserosa cells (aPKC, *n*=17/18 embryos; Baz, *n*=8/8 embryos).

Baz apicomedially in amnioserosa cells, and additionally it is important for Baz to promote aPKC localisation.

aPKC phosphorylation of Baz destabilises apicomedial aPKC-Baz complexes

The C-terminal aPKC-binding region in Baz contains a conserved serine (S980) that is phosphorylated by aPKC (Tepass, 2012). Phosphorylation of S980 by aPKC weakens aPKC-Baz binding (Morais-de-Sá et al., 2010). As our data implicated the aPKC-binding region in the apical localisation of Baz, we wondered how aPKC phosphorylation of Baz affects Par protein localisation and function during DC.

To assess the phosphorylation of Baz by aPKC, we immunostained embryos with an antibody specific for Baz phospho-S980 (Morais-de-Sá et al., 2010). During early DC, circumferential and apicomedial phopho-S980 was detected in amnioserosa cells (Fig. 5A). During later DC, amnioserosa apicomedial phospho-pS980 staining increased to levels comparable to that seen around the circumference of epidermal cells (Fig. 5A). To compare the detection of phospho-S980 with total Baz, we stained the Baz::GFP trap line (Fig. 5B). At early DC, there was substantial colocalisation between the two over the amnioserosa, but the degree of colocalisation decreased significantly when regions overlapping with circumferential DE-cad (Shotgun – FlyBase) staining were excluded from the analysis. At later DC, the overall degree of

amnioserosa colocalisation was indistinguishable from early DC, but when only the apicomedial distributions were compared, there was a significant increase from early to late DC. Thus, we detect Baz-aPKC interactions in the form of Baz phosphorylation in the amnioserosa, and notably, these interactions shift from the apical circumference to the apicomedial domain as DC proceeds.

To test how the aPKC phosphorylation site affects aPKC-Baz interactions in amnioserosa cells, we overexpressed either WT or mutant forms of Baz that abolished or mimicked S980 phosphorylation (S980A and S980E, respectively). In other cell types, non-phosphorylatable Baz[S980A] is known to have increased affinity for aPKC compared with Baz[S980E] or full-length Baz (Morais-de-Sá et al., 2010). In amnioserosa cells at DC, both Baz::GFP and Baz[S980E]::GFP localised to the apical circumference and apical surface of amnioserosa cells (Fig. 5C; supplementary material Fig. S1A,C). By contrast, Baz[S980A]::GFP localised predominantly to the apical surface of amnioserosa cells, where it accumulated in intense puncta (Fig. 5C; supplementary material Fig. S1A,C). Staining for aPKC revealed a dramatic and dose-dependent recruitment of aPKC to the Baz[S980A]::GFP puncta (Fig. 5C), suggesting that these puncta have similarities to large Baz[S980A]::GFP puncta that can be formed around the apical circumference of epidermal cells (Morais-de-Sá et al., 2010). The general ability of Baz[S980A]::GFP to recruit and accumulate aPKC was confirmed by expressing the construct in a striped pattern in the epidermis, whereas minimal or no effects were seen with
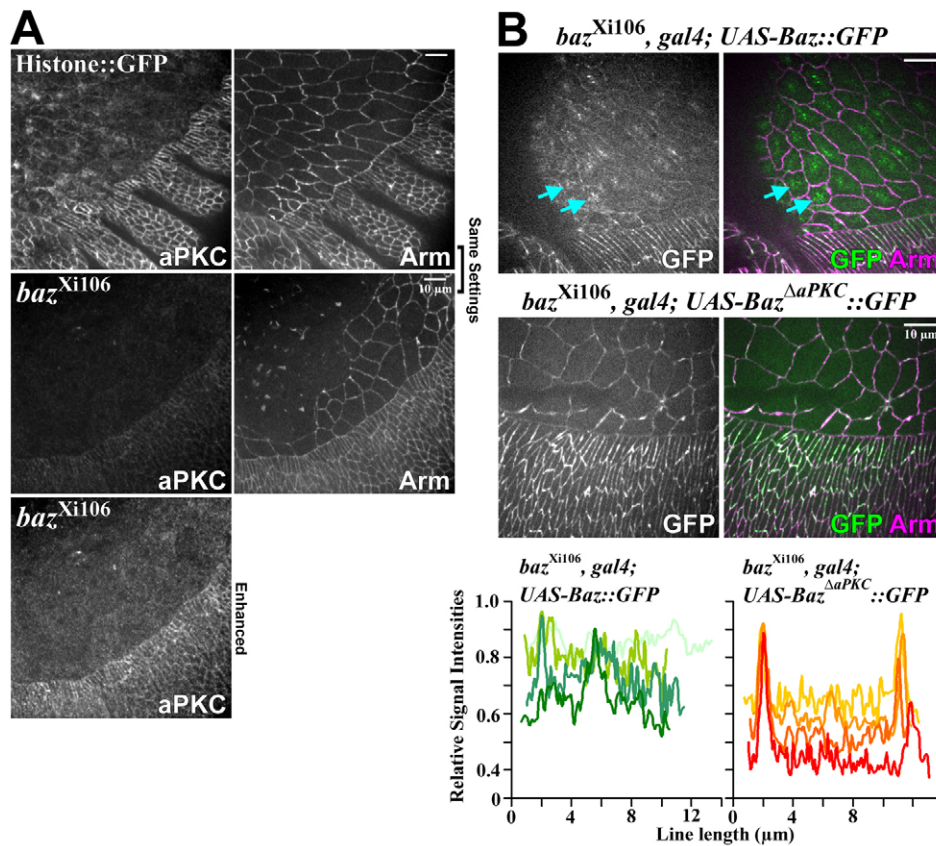
DEVELOPMENT

Fig. 4. The aPKC-binding region of Baz functions in apicomedial Baz recruitment.
(A) Reduced aPKC levels in baz[Xi106] zygotic mutant amnioserosa and epidermal cells. Upper four images collected with same settings. Lower image enhanced to show aPKC. Armadillo marks circumferences and shows region of amnioserosa breakdown in baz mutant. (B) Comparison of Baz::GFP and Baz[ΔaPKC]::GFP expressed in baz[Xi106] zygotic mutants. Amnioserosa Baz::GFP is apicomedial (arrows) but Baz[ΔaPKC]::GFP is circumferential. Armadillo marks circumferences. Quantification is shown below with line scans across single amnioserosa cell apical domains (n=4 embryos each; see Materials and methods).

Baz::GFP and Baz[S980E]::GFP, respectively (supplementary material Fig. S1C). Comparing the levels of Baz::GFP, Baz[S980A]::GFP and Baz[S980E]::GFP in the epidermis revealed that Baz[S980A]::GFP had the lowest expression levels of the three constructs (supplementary material Fig. S1A,B), and thus the effects of Baz[S980A]::GFP appear to be due to its non-phosphorylatable state. These data further implicate the aPKC-binding region in Baz in the recruitment of both Baz and aPKC to the apical surface of amnioserosa cells. More significantly, the phosphorylation of Baz by aPKC is crucial for reversing complex formation in the apicomedial domain of amnioserosa cells.

Stabilisation of apicomedial Baz-aPKC complexes leads to apical constriction

Because Baz and aPKC have opposing effects on the pulsing of apicomedial actomyosin networks (David et al., 2010), increasing Baz-aPKC interactions and the levels of each protein at the apicomedial domain allowed us to test if their effects on apical constriction are somehow linked. Thus, we compared the apical surface areas of amnioserosa cells overexpressing Baz[S980A]::GFP, Baz[S980E]::GFP, Baz::GFP or GFP. Amnioserosa cells expressing the highest levels of Baz[S980A]::GFP were consistently more constricted than cells in the same tissue with the lowest construct expression, and this induced constriction was only observed for this construct (Fig. 6A-D). We confirmed the specific effect of Baz[S980A]::GFP by measuring the apical surface areas of the eight highest expressing cells and the eight lowest expressing cells per embryo for each of the constructs. Only Baz[S980A]::GFP led to a significant difference in the apical surfaces areas between the two groups of cells (Fig. 6E; $P<0.05$, n=10 embryos). We considered the possibility that Baz[S980A]::GFP overexpression might be inducing apoptosis and apical constriction associated with delamination (Toyama et al., 2008), but we detected no cleaved caspase 3 in the constricted cells

(data not shown). Also, apoptotic cells undergo a relatively smooth (non-pulsatile) constriction process (Sokolow et al., 2012), whereas the cells induced to constrict by Baz[S980A]::GFP continually expanded and contracted (data not shown; we could not distinguish if these movements were due to cell autonomous contractile pulsations or due to the contractions of neighbouring cells with lower construct expression, e.g. actomyosin behaviour was not clearly revealed with co-imaging with Sqh-mCherry because of interference from intense cytoplasmic protein aggregates). Overall, these data indicate that stabilised Baz-aPKC interactions can induce apical constriction of amnioserosa cells. As aPKC is known to inhibit the actomyosin networks responsible for apical constriction, it appears that in cells expressing Baz[S980A]::GFP, the elevated apicomedial aPKC recruited by Baz[S980A]::GFP is inhibited from antagonising actomyosin, presumably because of its stabilised interactions with the Baz construct.

Gradual reductions of myosin inhibition dampen amnioserosa cell oscillations *in silico*

Because apicomedial Baz-aPKC interactions appear to increase over DC, we hypothesised that a gradual increase in the inhibition of aPKC by Baz would lead to a gradual decrease in the antagonism of actomyosin networks by aPKC and thus a stabilisation of the networks and a dampening of cell oscillations. To test if gradual reductions of myosin inhibitory factors would dampen cell oscillations, we turned to a recently developed mathematical model of DC (Wang et al., 2012). This model mechanically couples amnioserosa cells through passively elastic circumferential edges and apicomedial spokes, and kinetic equations describe myosin and signalling dynamics that control the assembly and action of myosin on the apicomedial spokes (summarised in Fig. 7B). With these components alone, amnioserosa cells continually oscillate (Fig. 7C; before 0 minutes). Mid-DC can be
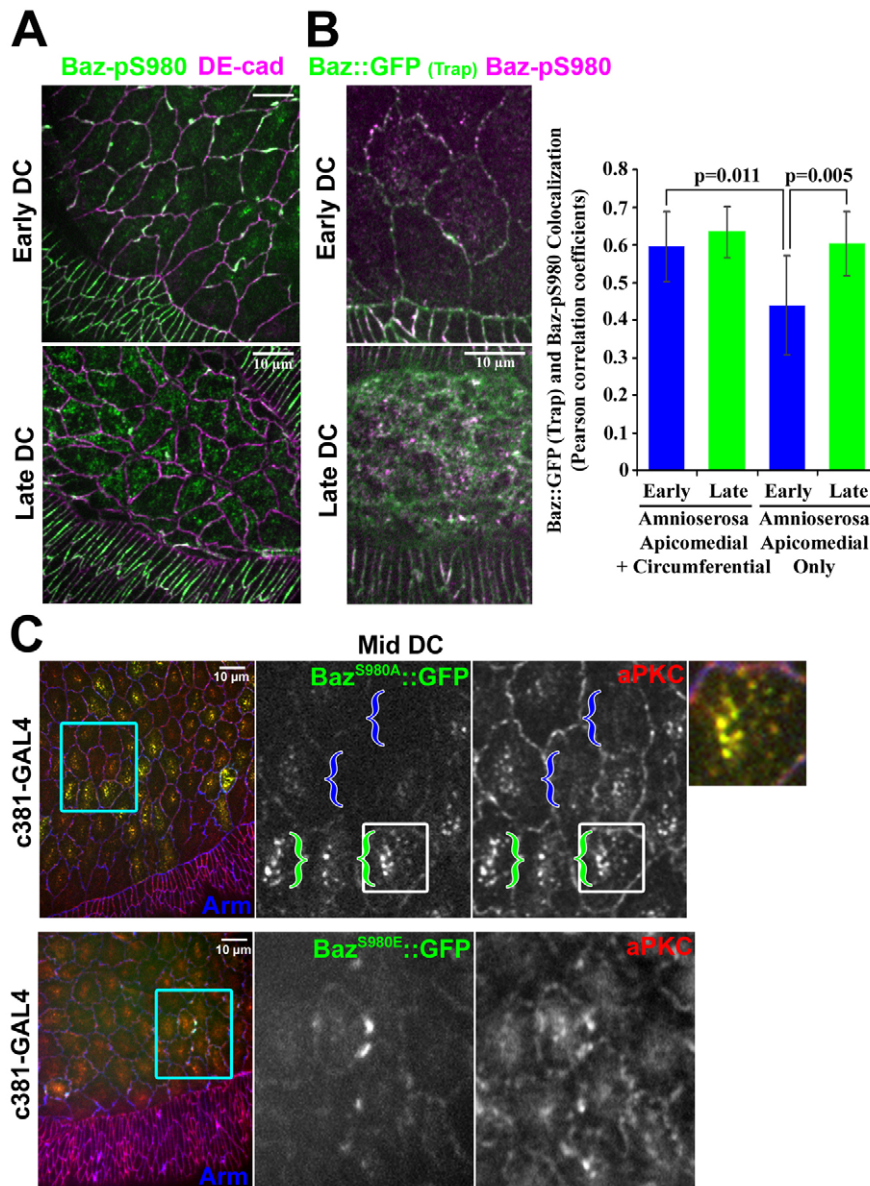
Fig. 5. Phosphorylation of the aPKC-binding region in Baz inhibits Baz-aPKC interactions in amnioserosa apicomedial domains.
(A) Phosphorylation of aPKC-binding region in Baz detected at early and late DC with a phospho-specific antibody in WT. (B) Comparisons of phospho-specific antibody staining with total Baz in the Baz::GFP trap line at early and late DC. Similar overall amnioserosa colocalisation was observed at both stages, but more apicomedial colocalisation was detected at late DC. Quantification is shown at the right (n=8 embryos for each stage). (C) Baz^{S980A}::GFP recruits aPKC and forms high intensity apicomedial puncta in amnioserosa cells. Baz^{S980E}::GFP has much milder effects on aPKC and its own accumulation. Turquoise boxes outline magnified regions in middle. White box outlines highly magnified region at far right. Blue and green brackets show cells with low and high Baz^{S980A}::GFP expression, respectively.

simulated by applying two ratchets: (1) an elastic, and continually shortening, cable around the perimeter of the entire tissue (an external ratchet), and (2) the continual shortening of edges and spokes inside each cell (an internal ratchet) (Wang et al., 2012) [Fig. 7C; simulation (0.5,0,0) after 0 minutes].

In the model, there are two parameters that inhibit myosin assembly onto spokes: (1) k_0 depletes an activating signal for myosin assembly, and (2) k_1 directly affects the myosin-spoke dissociation constant (Fig. 7B). Thus, we tested if gradual reductions of k_0 or k_1, or both, would dampen cell oscillations after mid-DC in the model. Starting at 0 minutes, the resting lengths of edges and spokes were decreased by 0.5% per average oscillation cycle, and additionally k_0 and k_1 were decreased by 0, 0.5 or 1% per cycle. The most striking dampening of cell oscillations occurred when both k_0 and k_1 were reduced [Fig. 7C; compare simulation (0.5,0,0) with (0.5,0.5,0.5), (0.5,0.5,1) and (0.5,1,1)]. Following 0 minutes, oscillations were initially similar to the control (which had no changes to k_0 or k_1), but abrupt dampening or loss of oscillations occurred between 50 and 100 minutes, in contrast to the control, in which oscillations continued. Similar trends were observed when the same changes to k_0 and k_1 were applied to

simulations undergoing 1.0% decreases of edge and spoke resting lengths per cycle, although these length changes alone dampened oscillations (supplementary material Fig. S2), and 2.0% length changes alone eliminated oscillations (data not shown). Of note, the reductions of myosin inhibition in the simulations did not lead to great reduction in cell area or to complete closure of the amnioserosa tissue, suggesting that elements of the model may be unnatural (e.g. the resistance of edges and spokes to compression) (Wang et al., 2012) or that elements are missing from the model (e.g. the effects of filopodial zippering) (Millard and Martin, 2008). Nonetheless, these simulations indicate that incremental and small reductions to myosin inhibition can lead to abrupt dampening of cell oscillations during DC.

DISCUSSION
Our data outline a regulatory circuit for guiding amnioserosa apical constriction (Fig. 7A). The circuit controls both the localisation and activity of its components. In terms of protein localisation, we find that amnioserosa actomyosin networks recruit the Par proteins to the apicomedial domain. Although Par protein puncta are not continually dependent on the actomyosin networks, their numbers
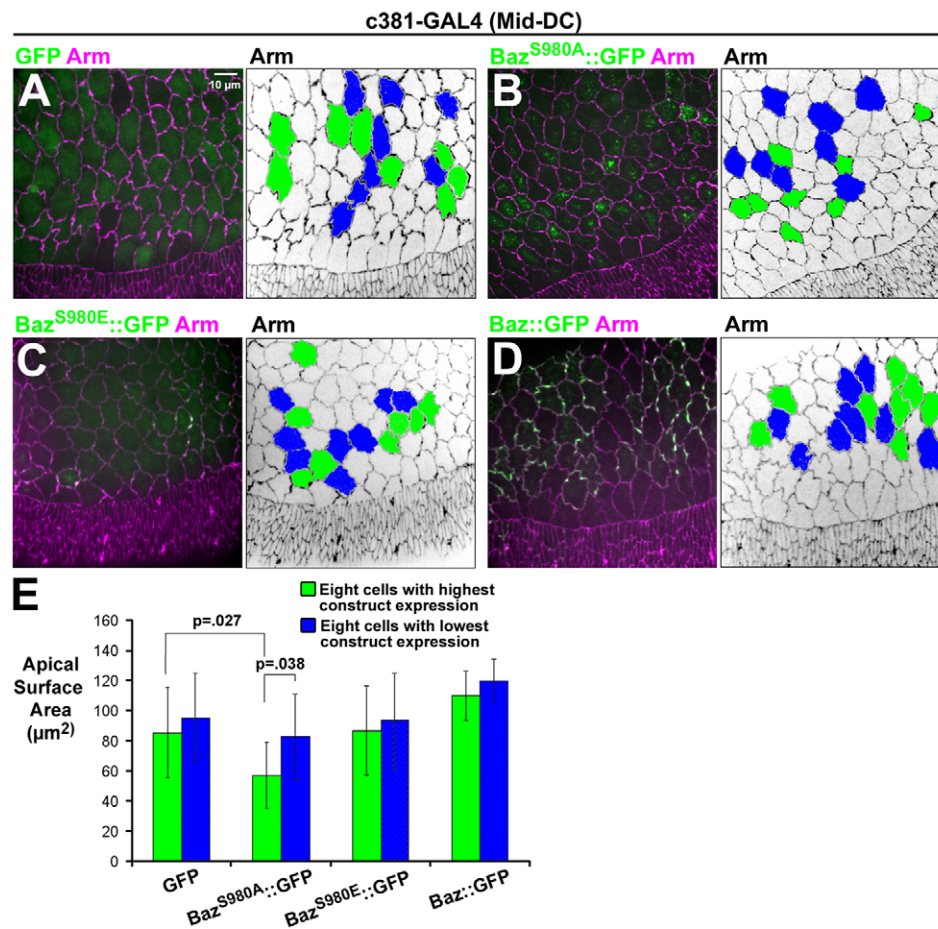
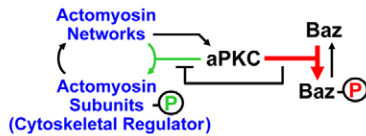**Fig. 6. Stabilised Baz-aPKC interactions promote apical constriction.**
(A-D) Amnioserosa expression of GFP (A), Baz[S980A]::GFP (B), Baz[S980E]::GFP (C) and Baz::GFP (D). Armadillo staining shows circumferences. Amnioserosa cells are at the top. The eight cells with lowest and highest construct expression are marked by blue and green, respectively. (E) Apical surface areas of the eight highest expressing cells and eight lowest expressing cells for GFP, Baz[S980A]::GFP, Baz[S980E]::GFP and Baz::GFP (mean ± s.d.; n=7-10 embryos each).

build over developmental time, apparently owing to the cumulative effect of multiple rounds of actomyosin network assembly. The networks appear to impact aPKC directly, and in turn, aPKC recruits Baz to the apical domain. This recruitment depends on the C-terminal aPKC-binding region of Baz, which aPKC phosphorylates for a dynamic relationship with Baz in the apical domain of amnioserosa cells.
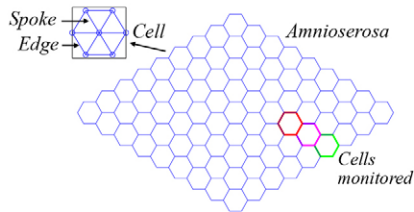
Par-6-aPKC activity inhibits amnioserosa actomyosin networks (David et al., 2010), and the recruitment of aPKC by the networks implicates a negative-feedback loop. As delayed negative feedback tied to a continual input signal can produce an oscillatory output (Ferrell et al., 2011; Lim et al., 2013), the actomyosin-aPKC negative-feedback loop might explain how aPKC regulates actomyosin network assembly-disassembly cycles (David et al., 2010). However, apical populations of Par-6-aPKC puncta are not fully recruited and fully removed with each actomyosin cycle, suggesting additional mechanisms. Importantly, Par-6-aPKC activity can be tempered by Baz. Thus, aPKC inhibition by Baz might delay the actomyosin-aPKC negative-feedback loop during early DC, promoting the actomyosin assembly-disassembly cycles. As DC proceeds, the additive effects of actomyosin assembly-disassembly cycles could increase apical Par protein levels; additionally, the gradual apical constriction of the cells decreases their apical surface areas and could thus increase apical surface Par protein concentrations. We propose that a gradual increase to apicomedial aPKC-Baz interactions inhibits aPKC and thus leads to the stabilisation of actomyosin networks. Our simulations indicate that this transition in network behaviour can occur abruptly following incremental reductions to myosin inhibition during earlier DC.

We propose that Baz acts as a competitive inhibitor to reduce aPKC phosphorylation of cytoskeletal regulators. This idea is consistent with reports of Par-3 inhibiting aPKC in kinase assays *in vitro* (Lin et al., 2000; Graybill et al., 2012). However, Baz is also known to promote aPKC localisation in the epidermis (Wodarz et al., 2000; Harris and Peifer, 2005) and amnioserosa (Fig. 4A). Thus, Baz appears to both promote and inhibit aPKC activity, potentially forming a paradoxical circuit (or incoherent feed-forward loop) (Hart and Alon, 2013; Lim et al., 2013) in which Baz and aPKC promote each other's recruitment, and in which Baz competitively inhibits aPKC activity. Significantly, Baz has multiple binding sites for the Par-6-aPKC complex [Par-6 binds Baz PDZ1 (Morais-de-Sá et al., 2010); aPKC binds Baz PDZ2-3 (Wodarz et al., 2000); aPKC binds the Baz C-terminal aPKC-binding region (Morais-de-Sá et al., 2010)], suggesting cooperative binding and that Baz interactions with the Par-6-aPKC complex are stronger than those between the Par-6-aPKC complex and its cytoskeleton targets. Notably, we find that Baz apical surface levels are ~66% lower than those of Par-6, suggesting that the inhibitory effect of Baz must be dynamic; Baz cannot simply sequester all Par-6-aPKC complexes by out-numbering them. The inhibitory effect must also depend on phosphatases because aPKC interactions with Baz are weakened following phosphorylation (Morais-de-Sá et al., 2010). Baz/Par-3 is known to be regulated by Protein phosphatase 1 (Traweger et al., 2008) and Protein phosphatase 2A (Krahn et al., 2009) with Protein phosphatase 1 de-phosphorylating the aPKC phosphorylation site of Par-3 (Traweger et al., 2008). Thus, Baz may act as a strong and dynamic inhibitor of Par-6-aPKC to buffer and eventually overcome the actomyosin-aPKC negative-feedback loop.

DEVELOPMENT

Fig. 7. Conceptual and mathematical models of the effect of Par proteins on each other, actomyosin networks and cell oscillations. (A) Proposed regulatory circuit connecting Par proteins and actomyosin networks. (B) Summary of mathematical model (for details, see Wang et al., 2012) and explanation of two parameters that inhibit myosin (k_0 and k_1). (C) Simulations of DC with internal and external ratchets activated at 0 minutes, along with no or various reductions in k_0 and k_1 per average oscillation cycle [(X,Y,Z):percentage reductions in spoke and edge resting lengths (X), k_0 (Y) and k_1 (Z) per average oscillation cycle]. The three curves are the normalised cell areas of the three cells marked in Fig. 7B. Cell oscillation often dampened abruptly following incremental k_0 and k_1 reductions (arrows). Unnatural instabilities occurred with greater k_1 reductions (asterisks).

A crucial unknown is the identity of the cytoskeletal target(s) of aPKC. Cytoskeletal targets of aPKC have been identified but have not been examined during amnioserosa apical constriction. In mammalian cells, Par-6-aPKC can phosphorylate Smurf1, an E3 ubiquitin ligase, in turn leading to RhoA degradation in cellular protrusions (Wang et al., 2003). During dendritic spine morphogenesis, Par-6-aPKC acts though p190RhoGAP to inhibit RhoA (Zhang and Macara, 2008). As well, aPKC phosphorylation of Rho kinase leads to its cortical dissociation in mammalian cell culture (Ishiuchi and Takeichi, 2011), and apparently during salivary gland tubulogenesis in *Drosophila* (Röper, 2012). Of note, the persistent Par-6-aPKC puncta could actively downregulate actomyosin activity, or prolong the lull between actomyosin activations, or do both. Another question is how actomyosin networks recruit aPKC. The recruitment of Par proteins by actomyosin networks has been documented during *Drosophila* cellularisation (Harris and Peifer, 2005) and *C. elegans* one-cell polarisation (Munro et al., 2004), and Baz and aPKC have been shown to co-immunoprecipitate with myosin regulatory light chain from *Drosophila* egg chambers (Wang and Riechmann, 2007), but specific linkages have yet to be identified. Defining further components of the actomyosin-aPKC negative-feedback loop will be crucial for understanding its regulation and its effects on actomyosin

network dynamics. In particular, despite identifying a potential delay mechanism for the loop, it is unclear how the loop and the delay mechanism could translate into oscillatory network behaviour. Perhaps the cytoskeletal target(s) of aPKC are co-recruited with the assembling networks, which in combination with the buffering effect of Baz, could delay their phosphorylation by aPKC. It is also possible that the clustering of Par protein puncta with each network assembly event could somehow modify the Baz buffering effect.

Another unanswered question is the influence of circumferential anchors for Baz or Par-6-aPKC, as weakening of these anchors could contribute to apicomedial Par protein accumulation over DC. Echinoid (Ed), a transmembrane AJ-associated protein that can directly bind Baz (Wei et al., 2005), is normally lost from the amnioserosa during DC (Laplante and Nilson, 2006; Laplante and Nilson, 2011). We hypothesised that this loss might promote the loss of Baz from AJs and its apicomedial accumulation. However, ectopic expression of Ed in the amnioserosa leading to circumferential Ed levels higher than those seen in the epidermis had no apparent effect on apicomedial Baz localisation (our unpublished observations). Thus, differences in Ed expression alone cannot account for the differential localisation of Par proteins between the amnioserosa and epidermis. It is possible that the effects of

actomyosin can overpower ectopic Ed, or that other changes to the apical circumference of amnioserosa cells are involved. More generally, other Par protein interaction partners should be considered. For example, Baz and Stardust also interact (Krahn et al., 2010) and, together with Crumbs and Patj, they form the apical Crumbs complex (Tepass, 2012). Recent results suggest Patj can activate myosin by suppressing myosin light chain phosphatase (Sen et al., 2012). Intriguingly, amnioserosa Baz^{S980A} apical surface puncta also recruit Patj (our unpublished observations), suggesting that this pathway might contribute to myosin activity as well.

In summary, our data argue that the differential regulation of amnioserosa actomyosin networks by Baz and Par-6-aPKC can be explained by a single pathway in which Baz inhibits Par-6-aPKC antagonism of the cytoskeletal networks. We also find that the actomyosin networks recruit aPKC, forming a negative-feedback loop. We propose that the inhibition of aPKC by Baz delays the negative feedback at earlier DC for cycling actomyosin networks, and with increased inhibition of aPKC by later DC, the actomyosin networks persist. These findings provide an example of how chemical signalling, and changes to this signalling, can modify the behaviour of actomyosin networks during embryo development.

MATERIALS AND METHODS

Fly stocks
yellow white and histone::GFP (gift from A. Wilde, University of Toronto, Canada) flies were wild-type and internal fixation controls. GFP gene traps into endogenous loci for zipper::GFP (CC01626) and Baz::GFP (CC01941) were from FlyTrap (Buszczak et al., 2007). GAL4 drivers were c381-Gal-4 [Bloomington *Drosophila* Stock Center (BDSC) 3734], daughterless-Gal-4 (BDSC 5460), paired-Gal-4 (BDSC 1947), and a baz^{Xi106}, maternal-α4-tubulin-Gal-4-VP16 recombinant chromosome (McKinley et al., 2012). UAS-constructs were UAS-CA-MLCK (Kim et al., 2002), UAS-Ed (Laplante and Nilson, 2011), UAS-Baz::GFP and UAS-Baz^{ΔaPKC}::GFP inserted into the attp2 integration site (McKinley et al., 2012), and Baz::GFP, Baz^{S980A}::GFP and Baz^{S980E}::GFP P-element insertions (Morais-de-Sá et al., 2010). Other stocks were: moeABD::GFP (Edwards et al., 1997), baz^{Xi106} (a gift from Andreas Wodarz, University of Gottingen, Germany), and a $par-6^{Δ226}$, Par-6::GFP genomic rescue line (Wirtz-Peitz et al., 2008).

Embryo staining
Embryos were dechorionated in 50% bleach for 5 minutes, washed in 0.1% Triton X-100, fixed in 1:1 3.7% formaldehyde in PBS:heptane for 20 minutes and methanol devitellinised. Embryos stained with phalloidin were fixed in 1:1 10% formaldehyde in PBS:heptane for 10 minutes and manually devitellinised. Blocking and staining were in PBS containing 1% goat serum, 1% sodium azide and 0.1% Triton X-100.

Primary antibodies were: mouse anti-Arm [1:350; Developmental Studies Hybridoma Bank (DSHB) N27A1]; rabbit anti-Baz (1:3500) (McKinley et al., 2012); rabbit anti-aPKC (1:1000; Santa Cruz Biotechnology C20), rabbit anti-Baz-pS980 (1:350; Morais-de-Sá et al., 2010); rat anti-DE-cad (1:100; DSHB DCAD2) and rat anti-Echinoid (1:100; Laplante and Nilson, 2011). F-actin was stained with Alexa Fluor 568-conjugated phalloidin (1:200; Invitrogen). Secondary antibodies were conjugated with Alexa Fluor 488, 546 or 647 (Invitrogen).

Pharmacological treatments
Embryos were dechorionated as above, rinsed twice in 0.9% NaCl, nutated in 1:1 octane:0.9% NaCl with DMSO or 10 μg/ml of cytochalasin D (Sigma-Aldrich) for 30 minutes at room temperature in the dark, and fixed as described above.

Imaging
Fixed samples were mounted in Aqua-Poly/Mount (Polysciences) and imaged with a Quorum spinning disk confocal system (Quorum

Technologies) at room temperature with a 40× (Plan-NeoFluar, NA 1.3) or 63× (Plan-Apochromat, NA 1.4) objective, a piezo top plate, a Hamamatsu EM CCD camera, Volocity software (Improvision), and z-stacks with 0.3-μm step sizes. For live imaging, dechorionated embryos were glued to coverslips, covered with halocarbon oil (series 700; Halocarbon Products), left open to the air, and imaged as described above. Egg shell vitelline membrane autofluorescence was a marker for the apical surface of underlying cells. Imaging for quantitative comparisons was performed on the same day with the same settings.

Post-acquisition analyses
Kymographs were created with ImageJ 1.46r (NIH).

To quantify puncta in the Baz::GFP Trap and Par-6::GFP rescue lines, individual puncta intensity sums were obtained in 3.3 μm^3 cubes (Imaris, Bitplane). Per embryo, two or three amnioserosa puncta measurements were taken and the background corrected by an average of three measurements taken outside the embryo. To measure apical surface puncta densities, 3.3-4.9 μm deep maximum intensity projections were made (Volocity). Regions of interest encompassing the maximum amnioserosa area available were thresholded (ImageJ) to select prominent apical circumferential and apicomedial puncta at early DC. These same thresholding parameters were applied to both stages, and the percentages of the amnioserosa areas occupied by the puncta were calculated.

To compare apical surface distributions of Baz::GFP and Baz^{ΔaPKC}::GFP in the baz^{Xi106} mutant background, line scans were obtained from four neighbouring rows of pixels across a single confocal section of a single amnioserosa cell apical domain (ImageJ). For each cell, the highest fluorescence intensity value was normalised to one, and the normalised intensities were averaged across the four lines and plotted.

To quantify aPKC apical surface enrichment in zip^1 mutants, mean fluorescence intensities within a box encompassing two or three amnioserosa cells were measured per z-section starting just above the apical domain and moving into the cell (ImageJ). For Baz, separate regions of interest were measured and averaged for each of four cells per embryo to avoid circumferential signals. For both proteins, measurements were normalised to the mean fluorescence intensity of the z-section 1.8 μm below the highest intensity apical surface section.

To quantify aPKC and Baz colocalisation with CA-MLCK-induced F-actin foci, signal and background levels within each channel were adjusted to match across the samples in single confocal sections. The three most prominent F-actin foci were selected per embryo, without evaluating aPKC or Baz. A region of interest was selected around the full apical surface (excluding the circumference) of each cell. Channels were compared using the ImageJ Colocalization Test.

To quantify phospho-S980 and Baz::GFP colocalisation, levels of single confocal sections were adjusted to match epidermal signal and background levels across the samples within each channel. Non-amnioserosa portions of the images were deleted and the Colocalization Test was applied. To exclude circumferential distributions, DE-cad staining was thresholded and subtracted from the phospho-S980 and Baz::GFP images (ImageJ).

Apical surface areas were measured following manual traces (ImageJ) of maximum intensity projections (Volocity). Highest and lowest GFP-expressing cells were determined by thresholding the data at different levels (ImageJ).

Statistical comparisons were carried out with unpaired two-tailed *t*-tests in Excel (Microsoft).

For figure preparation, input levels were adjusted in Adobe Photoshop while maintaining signal range over full output greyscale. Images were resized by bicubic interpolation with minimal changes at normal magnifications.

Competing interests
The authors declare no competing financial interests.

References
Blanchard, G. B., Murugesu, S., Adams, R. J., Martinez-Arias, A. and Gorfinkiel, N. (2010). Cytoskeletal dynamics and supracellular organisation of cell shape fluctuations during dorsal closure. *Development* **137**, 2743-2752.
Buszczak, M., Paterno, S., Lighthouse, D., Bachman, J., Planck, J., Owen, S., Skora, A. D., Nystul, T. G., Ohlstein, B., Allen, A. et al. (2007). The carnegie protein trap library: a versatile tool for Drosophila developmental studies. *Genetics* **175**, 1505-1531.
Chhabra, E. S. and Higgs, H. N. (2007). The many faces of actin: matching assembly factors with cellular structures. *Nat. Cell Biol.* **9**, 1110-1121.
David, D. J., Tishkina, A. and Harris, T. J. (2010). The PAR complex regulates pulsed actomyosin contractions during amnioserosa apical constriction in Drosophila. *Development* **137**, 1645-1655.
Edwards, K. A., Demsky, M., Montague, R. A., Weymouth, N. and Kiehart, D. P. (1997). GFP-moesin illuminates actin cytoskeleton dynamics in living tissue and demonstrates cell shape changes during morphogenesis in Drosophila. *Dev. Biol.* **191**, 103-117.
Ferrell, J. E., Jr, Tsai, T. Y. and Yang, Q. (2011). Modeling the cell cycle: why do certain circuits oscillate? *Cell* **144**, 874-885.
Franke, J. D., Montague, R. A. and Kiehart, D. P. (2005). Nonmuscle myosin II generates forces that transmit tension and drive contraction in multiple tissues during dorsal closure. *Curr. Biol.* **15**, 2208-2221.
Goldstein, B. and Macara, I. G. (2007). The PAR proteins: fundamental players in animal cell polarization. *Dev. Cell* **13**, 609-622.
Gorfinkiel, N. and Blanchard, G. B. (2011). Dynamics of actomyosin contractile activity during epithelial morphogenesis. *Curr. Opin. Cell Biol.* **23**, 531-539.
Graybill, C., Wee, B., Atwood, S. X. and Prehoda, K. E. (2012). Partitioning-defective protein 6 (Par-6) activates atypical protein kinase C (aPKC) by pseudosubstrate displacement. *J. Biol. Chem.* **287**, 21003-21011.
Guilgur, L. G., Prudêncio, P., Ferreira, T., Pimenta-Marques, A. R. and Martinho, R. G. (2012). Drosophila aPKC is required for mitotic spindle orientation during symmetric division of epithelial cells. *Development* **139**, 503-513.
Harris, T. J. (2012). Adherens junction assembly and function in the Drosophila embryo. *Int. Rev. Cell Mol. Biol.* **293**, 45-83.
Harris, T. J. and Peifer, M. (2005). The positioning and segregation of apical cues during epithelial polarity establishment in Drosophila. *J. Cell Biol.* **170**, 813-823.
Harris, T. J. and Peifer, M. (2007). aPKC controls microtubule organization to balance adherens junction symmetry and planar polarity during development. *Dev. Cell* **12**, 727-738.
Hart, Y. and Alon, U. (2013). The utility of paradoxical components in biological circuits. *Mol. Cell* **49**, 213-221.
Ishiuchi, T. and Takeichi, M. (2011). Willin and Par3 cooperatively regulate epithelial apical constriction through aPKC-mediated ROCK phosphorylation. *Nat. Cell Biol.* **13**, 860-866.
Kim, Y. S., Fritz, J. L., Seneviratne, A. K. and VanBerkum, M. F. (2002). Constitutively active myosin light chain kinase alters axon guidance decisions in Drosophila embryos. *Dev. Biol.* **249**, 367-381.
Krahn, M. P., Egger-Adam, D. and Wodarz, A. (2009). PP2A antagonizes phosphorylation of Bazooka by PAR-1 to control apical-basal polarity in dividing embryonic neuroblasts. *Dev. Cell* **16**, 901-908.
Krahn, M. P., Bückers, J., Kastrup, L. and Wodarz, A. (2010). Formation of a Bazooka-Stardust complex is essential for plasma membrane polarity in epithelia. *J. Cell Biol.* **190**, 751-760.
Kruse, K. and Riveline, D. (2011). Spontaneous mechanical oscillations: implications for developing organisms. *Curr. Top. Dev. Biol.* **95**, 67-91.
Laplante, C. and Nilson, L. A. (2006). Differential expression of the adhesion molecule Echinoid drives epithelial morphogenesis in Drosophila. *Development* **133**, 3255-3264.
Laplante, C. and Nilson, L. A. (2011). Asymmetric distribution of Echinoid defines the epidermal leading edge during Drosophila dorsal closure. *J. Cell Biol.* **192**, 335-348.
Levayer, R. and Lecuit, T. (2012). Biomechanical regulation of contractility: spatial control and dynamics. *Trends Cell Biol.* **22**, 61-81.
Lim, W. A., Lee, C. M. and Tang, C. (2013). Design principles of regulatory networks: searching for the molecular algorithms of the cell. *Mol. Cell* **49**, 202-212.
Lin, D., Edwards, A. S., Fawcett, J. P., Mbamalu, G., Scott, J. D. and Pawson, T. (2000). A mammalian PAR-3-PAR-6 complex implicated in Cdc42/Rac1 and aPKC signalling and cell polarity. *Nat. Cell Biol.* **2**, 549-552.
Martin, A. C. (2010). Pulsation and stabilization: contractile forces that underlie morphogenesis. *Dev. Biol.* **341**, 114-125.
Martin, A. C., Kaschube, M. and Wieschaus, E. F. (2009). Pulsed contractions of an actin-myosin network drive apical constriction. *Nature* **457**, 495-499.
McKinley, R. F., Yu, C. G. and Harris, T. J. (2012). Assembly of Bazooka polarity landmarks through a multifaceted membrane-association mechanism. *J. Cell Sci.* **125**, 1177-1190.
Millard, T. H. and Martin, P. (2008). Dynamic analysis of filopodial interactions during the zippering phase of Drosophila dorsal closure. *Development* **135**, 621-626.
Morais-de-Sá, E., Mirouse, V. and St Johnston, D. (2010). aPKC phosphorylation of Bazooka defines the apical/lateral border in Drosophila epithelial cells. *Cell* **141**, 509-523.
Mortensen, K. and Larsson, L. I. (2003). Effects of cytochalasin D on the actin cytoskeleton: association of neoformed actin aggregates with proteins involved in signaling and endocytosis. *Cell. Mol. Life Sci.* **60**, 1007-1012.
Munro, E., Nance, J. and Priess, J. R. (2004). Cortical flows powered by asymmetrical contraction transport PAR proteins to establish and maintain anterior-posterior polarity in the early C. elegans embryo. *Dev. Cell* **7**, 413-424.
Pollard, T. D. (2007). Regulation of actin filament assembly by Arp2/3 complex and formins. *Annu. Rev. Biophys. Biomol. Struct.* **36**, 451-477.
Roh-Johnson, M., Shemer, G., Higgins, C. D., McClellan, J. H., Werts, A. D., Tulu, U. S., Gao, L., Betzig, E., Kiehart, D. P. and Goldstein, B. (2012). Triggering a cell shape change by exploiting preexisting actomyosin contractions. *Science* **335**, 1232-1235.
Rolls, M. M., Albertson, R., Shih, H. P., Lee, C. Y. and Doe, C. Q. (2003). Drosophila aPKC regulates cell polarity and cell proliferation in neuroblasts and epithelia. *J. Cell Biol.* **163**, 1089-1098.
Röper, K. (2012). Anisotropy of Crumbs and aPKC drives myosin cable assembly during tube formation. *Dev. Cell* **23**, 939-953.
Sawyer, J. M., Harrell, J. R., Shemer, G., Sullivan-Brown, J., Roh-Johnson, M. and Goldstein, B. (2010). Apical constriction: a cell shape change that can drive morphogenesis. *Dev. Biol.* **341**, 5-19.
Schliwa, M. (1982). Action of cytochalasin D on cytoskeletal networks. *J. Cell Biol.* **92**, 79-91.
Sen, A., Nagy-Zsvér-Vadas, Z. and Krahn, M. P. (2012). Drosophila PATJ supports adherens junction stability by modulating Myosin light chain activity. *J. Cell Biol.* **199**, 685-698.
Sokolow, A., Toyama, Y., Kiehart, D. P. and Edwards, G. S. (2012). Cell ingression and apical shape oscillations during dorsal closure in Drosophila. *Biophys. J.* **102**, 969-979.
Solon, J., Kaya-Copur, A., Colombelli, J. and Brunner, D. (2009). Pulsed forces timed by a ratchet-like mechanism drive directed tissue movement during dorsal closure. *Cell* **137**, 1331-1342.
St Johnston, D. and Ahringer, J. (2010). Cell polarity in eggs and epithelia: parallels and diversity. *Cell* **141**, 757-774.
Suzuki, M., Morita, H. and Ueno, N. (2012). Molecular mechanisms of cell shape changes that contribute to vertebrate neural tube closure. *Dev. Growth Differ.* **54**, 266-276.
Tanentzapf, G. and Tepass, U. (2003). Interactions between the crumbs, lethal giant larvae and bazooka pathways in epithelial polarization. *Nat. Cell Biol.* **5**, 46-52.
Tepass, U. (2012). The apical polarity protein network in Drosophila epithelial cells: regulation of polarity, junctions, morphogenesis, cell growth, and survival. *Annu. Rev. Cell Dev. Biol.* **28**, 655-685.
Toyama, Y., Peralta, X. G., Wells, A. R., Kiehart, D. P. and Edwards, G. S. (2008). Apoptotic force and tissue dynamics during Drosophila embryogenesis. *Science* **321**, 1683-1686.
Traweger, A., Wiggin, G., Taylor, L., Tate, S. A., Metalnikov, P. and Pawson, T. (2008). Protein phosphatase 1 regulates the phosphorylation state of the polarity scaffold Par-3. *Proc. Natl. Acad. Sci. USA* **105**, 10402-10407.
Wang, Y. and Riechmann, V. (2007). The role of the actomyosin cytoskeleton in coordination of tissue growth during Drosophila oogenesis. *Curr. Biol.* **17**, 1349-1355.
Wang, H. R., Zhang, Y., Ozdamar, B., Ogunjimi, A. A., Alexandrova, E., Thomsen, G. H. and Wrana, J. L. (2003). Regulation of cell polarity and protrusion formation by targeting RhoA for degradation. *Science* **302**, 1775-1779.
Wang, Q., Feng, J. J. and Pismen, L. M. (2012). A cell-level biomechanical model of Drosophila dorsal closure. *Biophys. J.* **103**, 2265-2274.
Wei, S. Y., Escudero, L. M., Yu, F., Chang, L. H., Chen, L. Y., Ho, Y. H., Lin, C. M., Chou, C. S., Chia, W., Modolell, J. et al. (2005). Echinoid is a component of adherens junctions that cooperates with DE-Cadherin to mediate cell adhesion. *Dev. Cell* **8**, 493-504.
Wirtz-Peitz, F., Nishimura, T. and Knoblich, J. A. (2008). Linking cell cycle to asymmetric division: Aurora-A phosphorylates the Par complex to regulate Numb localization. *Cell* **135**, 161-173.
Wodarz, A., Ramrath, A., Grimm, A. and Knust, E. (2000). Drosophila atypical protein kinase C associates with Bazooka and controls polarity of epithelia and neuroblasts. *J. Cell Biol.* **150**, 1361-1374.
Zhang, H. and Macara, I. G. (2008). The PAR-6 polarity protein regulates dendritic spine morphogenesis through p190 RhoGAP and the Rho GTPase. *Dev. Cell* **14**, 216-226.

DEVELOPMENT